



UNIVERSITY OF LEEDS

This is a repository copy of *Dykes as physical buffers to metamorphic overprinting: an example from the Archaean–Palaeoproterozoic Lewisian Gneiss Complex of NW Scotland*.

White Rose Research Online URL for this paper:
<http://eprints.whiterose.ac.uk/137087/>

Version: Accepted Version

Article:

MacDonald, JM, Magee, C orcid.org/0000-0001-9836-2365 and Goodenough, KM (2017) Dykes as physical buffers to metamorphic overprinting: an example from the Archaean–Palaeoproterozoic Lewisian Gneiss Complex of NW Scotland. *Scottish Journal of Geology*, 53 (2). pp. 41-52. ISSN 0036-9276

<https://doi.org/10.1144/sjg2017-004>

© 2017 The Author(s). This is an author produced version of a paper published in *Scottish Journal of Geology*. Uploaded in accordance with the publisher's self-archiving policy.

Reuse

Items deposited in White Rose Research Online are protected by copyright, with all rights reserved unless indicated otherwise. They may be downloaded and/or printed for private study, or other acts as permitted by national copyright laws. The publisher or other rights holders may allow further reproduction and re-use of the full text version. This is indicated by the licence information on the White Rose Research Online record for the item.

Takedown

If you consider content in White Rose Research Online to be in breach of UK law, please notify us by emailing eprints@whiterose.ac.uk including the URL of the record and the reason for the withdrawal request.



eprints@whiterose.ac.uk
<https://eprints.whiterose.ac.uk/>

Scottish Journal of Geology

Dykes as buffers to metamorphic overprinting: an example from the Archaean-Palaeoproterozoic Lewisian Gneiss Complex of Northwest Scotland --Manuscript Draft--

Manuscript Number:	
Article Type:	Research article
Full Title:	Dykes as buffers to metamorphic overprinting: an example from the Archaean-Palaeoproterozoic Lewisian Gneiss Complex of Northwest Scotland
Short Title:	Dykes as buffers to metamorphic overprinting
Corresponding Author:	John MacDonald University of Glasgow UNITED KINGDOM
Corresponding Author E-Mail:	john.macdonald.3@glasgow.ac.uk
Other Authors:	Craig Magee Kathryn Goodenough
Abstract:	<p>The early history of polymetamorphic basement gneiss complexes is often difficult to decipher due to overprinting by later deformation and metamorphism. The Archaean tonalite-trondhjemite-granodiorite (TTG) gneisses of the Lewisian Gneiss Complex are cut by the Palaeoproterozoic (~2400 Ma) Scourie Dyke Swarm and both are deformed by later shear zones developed during the amphibolite-facies Laxfordian event (1740-1670 Ma). Detailed field mapping, petrographic analysis and mineral chemistry reveal that the xenolith of TTG gneiss entrained within a Scourie Dyke has been protected from amphibolite-facies recrystallization in a Laxfordian shear zone. Whilst surrounding TTG gneiss displays pervasive amphibolite-facies retrogression, the xenolith retains a pre-Scourie Dyke, granulite-facies metamorphic assemblage and gneissic layering. We suggest that retrogressive reaction softening and pre-existing planes of weakness, such as the ~2490 Ma Inverian fabric and gneiss-dyke contacts, localised strain around but not within the xenolith. Such strain localisation could generate preferential flow pathways for fluids, principally along the shear zone, bypassing the xenolith and protecting it from amphibolite-facies retrogression. In basement gneiss complexes where early metamorphic assemblages and fabrics have been fully overprinted by tectonothermal events, our results suggest that country rock xenoliths in mafic dykes could preserve windows into the early evolution of these complex polymetamorphic areas.</p>
Manuscript Classifications:	Geochemistry; Metamorphic geology; Structural geology
Additional Information:	
Question	Response
Are there any conflicting interests, financial or otherwise?	No
Samples used for data or illustrations in this article have been collected in a responsible manner	Confirmed
Author Comments:	
Suggested Reviewers:	Tim Johnson Curtin University Tim.Johnson@curtin.edu.au currently active in Lewisian geology Mark Pearce CSIRO Mark.Pearce@csiro.au relatively recently working on Lewisian, particularly field/metamorphism aspects

Opposed Reviewers:

1 **Dykes as buffers to metamorphic overprinting: an example from the**
2 **Archaean-Palaeoproterozoic Lewisian Gneiss Complex of Northwest Scotland**

3

4 J. M. MACDONALD^{1,*}, C. MAGEE² AND K. M. GOODENOUGH³

5 ¹*Department of Earth, Ocean & Ecological Sciences, University of Liverpool, Liverpool, L69 3GP, UK*

6 ²*Department of Earth Science & Engineering, Imperial College London, London, SW7 2AZ, UK*

7 ³*British Geological Survey, Research Avenue South, Edinburgh, EH14 4AP, UK*

8 **Present address: School of Geographical & Earth Sciences, University of Glasgow, Glasgow, G12*

9 *8QQ, UK. john.macdonald.3@glasgow.ac.uk*

10

11

12

13

14

15

16

17

18

19

20

21

22

23

24

25

26 **ABSTRACT**

27

28 The early history of polymetamorphic basement gneiss complexes is often difficult to decipher due
29 to overprinting by later deformation and metamorphic events. In this paper, we integrate field,
30 petrographic and mineral chemistry data from an Archaean tonalitic gneiss xenolith hosted within a
31 Palaeoproterozoic mafic dyke in the Lewisian Gneiss Complex of NW Scotland to show how xenoliths
32 in dykes may preserve signatures of early tectonothermal histories. The Archaean tonalite-
33 trondhjemite-granodiorite (TTG) gneisses of the Lewisian Gneiss Complex are cut by a suite of
34 Palaeoproterozoic (~2400 Ma) mafic dykes, the Scourie Dyke Swarm, and both are deformed by later
35 shear zones developed during the amphibolite-facies Laxfordian event (1740-1670 Ma). Detailed
36 field mapping, petrographic analysis and mineral chemistry reveal that the xenolith of TTG gneiss
37 entrained within a Scourie Dyke has been protected from amphibolite-facies recrystallization in a
38 Laxfordian shear zone. Whilst surrounding TTG gneiss displays pervasive amphibolite-facies
39 retrogression, the xenolith retains a pre-Scourie Dyke, granulite-facies metamorphic assemblage and
40 gneissic layering. We suggest that retrogressive reaction softening and pre-existing planes of
41 weakness, such as the ~2490 Ma Inverian fabric and gneiss-dyke contacts, localised strain around
42 but not within the xenolith. Such strain localisation could generate preferential flow pathways for
43 fluids, principally along the shear zone, bypassing the xenolith and protecting it from amphibolite-
44 facies retrogression. In basement gneiss complexes where early metamorphic assemblages and
45 fabrics have been fully overprinted by tectonothermal events, our results suggest that country rock
46 xenoliths in mafic dykes could preserve windows into the early evolution of these complex
47 polymetamorphic areas.

48

49 **Key words:** metamorphic overprinting; mafic dyke; buffer; TTG gneiss; xenolith

50

51

52 INTRODUCTION

53 Unravelling the geological history of polymetamorphic basement gneiss complexes is often
54 difficult because older tectonothermal events are commonly overprinted by younger metamorphism
55 and deformation. In particular, recrystallisation of the rock to form new mineral fabrics and
56 metamorphic assemblages can obliterate older fabrics and mineral assemblages related to early
57 tectonothermal events. Thermal resetting can also overprint isotopic and trace element signatures in
58 petrogenetic indicator minerals such as zircon (e.g. Hoskin & Schaltegger, 2003). These processes
59 may therefore obscure our understanding of early tectonothermal events. However, complete
60 overprinting does not always occur. For example, phenomena such as reaction softening and strain
61 localisation can result in spatially heterogeneous tectonothermal overprinting (e.g. White, 2004;
62 Olliot, *et al.*, 2010). This is because structures generated by reaction softening and strain localisation
63 (e.g. shear zones) may channel fluid flow, which is required for metamorphic reactions occurring in
64 the amphibolite-facies, promoting heterogeneous tectonothermal overprinting (e.g. White & Knipe,
65 1978).

66 To investigate potential controls on heterogeneous overprinting, we present field,
67 petrographic and geochemical evidence from the polymetamorphic tonalite-trondhjemite-
68 granodiorite (TTG) Archaean gneisses of the Lewisian Gneiss Complex of Northwest Scotland (Fig.
69 1a). This work suggests that igneous intrusions may impede post-entrapment metamorphism and
70 deformation of gneissic country rock xenoliths. In the Assynt Terrane (Kinny, *et al.*, 2005) of the
71 Lewisian Gneiss Complex (Fig. 1a), the location of this study, field evidence shows that the TTG
72 gneisses have undergone three tectonothermal events: (i) an initial granulite-facies metamorphism
73 with formation of gneissic layering (the Badcallian event); (ii) an amphibolite-facies metamorphism
74 with formation of shear zones several kilometres wide (the Inverian event) followed by mafic dyke
75 intrusion; and (iii) a final amphibolite-facies metamorphism with formation of shear zones tens of
76 metres wide (the Laxfordian event) (e.g. Sutton & Watson, 1951; Evans, 1965; Park, 1970; Wynn,
77 1995). We examine a TTG xenolith, within a Scourie Dyke, that is characterised by an early gneissic

78 layering and granulite-facies mineral assemblage, despite being entrained within a dyke that is
79 deformed and metamorphosed by a shear zone formed during the Laxfordian event.

80

81 **GEOLOGICAL SETTING**

82 The Archaean-Palaeoproterozoic Lewisian Gneiss Complex, located in Northwest Scotland (Fig. 1a), is
83 predominantly composed of tonalite-trondhjemite-granodiorite (TTG) gneiss, with abundant small
84 bodies of mafic gneiss and sparse larger mafic bodies metasedimentary gneisses (e.g. Peach, *et al.*,
85 1907; Tarney & Weaver, 1987). Early mapping of structures and metamorphic mineral assemblages
86 by Sutton and Watson (1951) led to the recognition of two tectonothermal events, temporally
87 separated by the emplacement at ~2400 Ma (Davies & Heaman, 2014) of a suite of mafic dykes
88 known as the Scourie Dyke Swarm. Subsequent work has shown that the pre-dyke tectonothermal
89 event can be subdivided into a gneiss-forming, granulite-facies event (the Badcallian; Park, 1970)
90 and a younger amphibolite-facies event (the Inverian; Evans, 1965). The Badcallian is characterised
91 by a generally flat-lying gneissic layering and a granulite-facies assemblage of plagioclase,
92 clinopyroxene, orthopyroxene and quartz in the TTG gneisses. There has been much debate over the
93 age of the Badcallian tectonothermal event (Friend & Kinny, 1995; Park, 2005; Crowley, *et al.*, 2014)
94 but is now generally accepted to have occurred at ~2700 Ma (Crowley, *et al.*, 2014). A major fluid
95 influx in the ~2490 Ma (Crowley, *et al.*, 2014) Inverian tectonothermal event resulted in widespread
96 hydrous retrogression of Badcallian pyroxenes to hornblende. Major shear zones up to ten
97 kilometres wide were formed, such as the Laxford Shear Zone (Goodenough, *et al.*, 2010) (Fig. 1b),
98 while the areas between these major shear zones underwent partial static retrogression (e.g. Beach,
99 1974).

100 Both the Badcallian and Inverian are heterogeneously overprinted by a post-dyke
101 tectonothermal event, the Laxfordian, and are only preserved in certain areas of the complex, most
102 notably the Assynt Terrane (Fig. 1b) (Kinny, *et al.*, 2005). Throughout much of the Lewisian Gneiss
103 Complex, the Laxfordian is characterised by pervasive deformation at lower amphibolite facies (e.g.

104 Sutton & Watson, 1951; Park, *et al.*, 1987). In contrast, the Laxfordian event in the Assynt Terrane is
105 represented by numerous discrete tens-of-metres-wide shear zones (e.g. Wynn, 1995; MacDonald,
106 *et al.*, 2013; MacDonald, *et al.*, 2015b) dated at c. 1740 Ma and 1670 Ma (Kinny, *et al.*, 2005), as well
107 as extension-related alkaline granite sheets at c. 1880 Ma and compression/partial melting granite
108 sheets at c. 1770 Ma (Goodenough, *et al.*, 2013). Because of the localised nature of Laxfordian
109 deformation, metamorphic assemblages and deformation fabrics of the earlier Badcallian and
110 Inverian tectonothermal events are locally preserved between these Laxfordian shear zones.

111

112 **RESULTS**

113 **FIELD RELATIONSHIPS**

114 The field area for this study is located to the north of Loch a' Phreasain Challtuinne (NC 188 467;
115 British National Grid) (Fig. 1c). This locality is within the Laxford Shear Zone, a ~5 km-wide shear zone
116 formed during the Inverian tectonothermal event and reactivated during the Laxfordian
117 tectonothermal event as multiple smaller shear zones that are tens of metres wide (Goodenough, *et*
118 *al.*, 2010). The margin of the Laxford Shear Zone is marked by a change from shallow-lying,
119 moderately-developed Badcallian gneissic layering of the country rock to more steeply dipping,
120 planar Inverian layering. The nearest pristine pyroxene-bearing granulite-facies Badcallian gneisses
121 are located several kilometres to the southwest of the study area, e.g. around Scourie (e.g. Sutton &
122 Watson, 1951; Johnson & White, 2011; MacDonald, *et al.*, 2015a). We conducted detailed mapping
123 of a small part of the Laxford Shear Zone encompassing the polyphase deformation history of the
124 area.

125 At the studied locality, a north-south oriented relatively planar Scourie Dyke, ~50 m wide,
126 cross-cuts layering in the TTG gneiss at angles of up to 90° (e.g., NC18919 46689 and NC 18906
127 46735; Fig. 2). This TTG layering is characterised by fine (~5-10 mm thick), alternating layers of felsic
128 and mafic minerals dipping at c. 70° to the SW. Weak mineral aggregate lineations of hornblende or
129 quartz are also sparsely developed in the TTG gneiss. Both the planar and linear fabrics here are

130 considered to be Inverian in age as they are associated with pyroxene-absent amphibolite-facies
131 mineralogy, but are cross-cut by the Scourie Dyke and are located within the Inverian section of the
132 Laxford Shear Zone mapped by Goodenough et al., (2010). The dyke is coarse-grained and composed
133 of equant hornblende crystals with interstitial plagioclase.

134 Around NC 1889 4675, the dyke is deflected to a WNW-ESE orientation and deformed by a
135 narrow Laxfordian shear zone (Figure 2). A strong fabric of plagioclase aggregates is developed
136 within the dyke, parallel to the planar fabric in the TTG gneisses. Within this narrow Laxfordian shear
137 zone, layering in the gneisses is flaggy with quartz and plagioclase aggregate lineations dipping at c.
138 5° WNW. The dyke contains discrete zones of a well-developed L-S tectonite fabric (e.g., NC 18838
139 46814; Fig. 3a), defined by aggregates of amphibole and/or plagioclase, clearly distinguishable from
140 the tectonically undeformed dyke outside the Laxfordian shear zone. The dip and strike of the planar
141 fabric is subparallel to the dyke-contact and dips >40° to the southwest. The transition in fabric style
142 within the dyke is gradational over approximately 5 m and is characterised by the progressive
143 elongation of anhedral, interstitial plagioclase into a zone where both hornblende and plagioclase
144 form a strong L-S tectonite fabric (Fig. 3b). The offset of the dyke across the shear zone is sinistral
145 and this is in accord with the observation of Wynn (1995) and published mapping
146 (BritishGeologicalSurvey, 2007). In the TTG gneisses, both the Inverian and Laxfordian planar fabrics
147 dip at c. 60-70° to the southwest, suggesting Laxfordian deformation reactivated the earlier Inverian
148 fabric.

149 Where the dyke is displaced by the Laxfordian shear zone, it contains four xenolithic masses
150 of TTG gneiss (Fig. 2). These bodies are referred to as xenoliths because they do not have the same
151 Inverian amphibolite-facies metamorphic assemblage as the country rock surrounding the dyke. The
152 largest and southernmost of these xenoliths has an elliptical plan-view morphology and is c. 60 × 15
153 m in size with its long axis parallel to the dyke margins. Around this xenolith the Scourie Dyke
154 displays a Laxfordian L-S tectonite fabric. However, only the outermost c. 1 m of the TTG gneiss
155 xenolith has a dyke-contact parallel flaggy fabric (Fig. 3c), interpreted to be Laxfordian. The majority

156 of the xenolith contains moderately well-developed gneissic layering which is defined by 5-20 mm
157 wide layers of mafic and felsic minerals, consistent with Badcallian gneissic layering (Fig. 3c);
158 clinopyroxene is abundant and is indicative of a Badcallian assemblage as it is not found in Inverian
159 assemblages in the Lewisian Gneiss Complex. This TTG gneiss xenolith enclosed within the Scourie
160 Dyke therefore appears to have been transported to its current location and largely escaped
161 overprinting, despite its position in a Laxfordian shear zone. In order to investigate this further,
162 samples for petrographic and mineral chemistry analysis were collected from the: (i) xenolith; (ii)
163 deformed and (iii) undeformed Scourie Dyke; (iv) TTG gneiss in the Laxfordian shear zone; and (v)
164 TTG gneiss away from the shear zone with the Inverian planar fabric.

165

166 **PETROGRAPHY**

167 **Sample JM08/32 (NC 18904 46681) – TTG gneiss with Inverian fabric**

168 Sample JM08/32 is composed of c. 50% quartz, c. 30% plagioclase, c. 10% hornblende, and c. 10%
169 biotite. Accessory opaque minerals are commonly spatially associated with biotite. The plagioclase
170 crystals are subhedral, up to 2 mm long, with occasional lamellar twinning and zoned extinction. The
171 quartz crystals are up to 0.5 mm in diameter and locally aggregate to form a linear fabric (Fig. 4a).
172 Hornblende occurs together with quartz in a sieve-texture, suggesting it has replaced pyroxene. In
173 places these pseudomorphs are elongate parallel to the quartz aggregate linear fabric (Fig. 4b).
174 Biotite laths are commonly clumped together but only very weakly align with the quartz fabric (Fig.
175 4c). The quartz aggregate lineation and elongated hornblende and quartz pseudomorphs were
176 formed during the Inverian event (Coward & Park, 1987; Goodenough, et al., 2010).

177

178 **Sample JM08/28 (NC 18919 46696) – Undeformed Scourie Dyke**

179 Sample JM08/28 is composed of c. 65% hornblende, c. 30% plagioclase and c. 5% quartz with
180 accessory opaque minerals. The hornblende occurs dominantly in a sieve texture with quartz,

181 indicating replacement of igneous pyroxene. These pseudomorphs are generally c. 2 mm in diameter
182 and have rims of hornblende aggregates with hornblende 'sieving' sub-millimetre rounded quartz
183 crystals in the centre (Fig. 4d). Clinopyroxene cores are locally preserved within the pseudomorphs.
184 Plagioclase forms 1-2 mm subhedral-to-anhedral crystals with well-preserved albite-pericline
185 lamellar twinning and zoned extinction (Fig. 4e). As well as occurring in a sieve texture with
186 hornblende, minor sub-millimetre anhedral quartz crystals are also found in the matrix. The lack of
187 any planar or linear fabrics show that this sample of Scourie Dyke has not been deformed but the
188 sieve-textured hornblende and quartz replacing igneous pyroxene demonstrates that it has been
189 statically retrogressed in the Laxfordian.

190

191 **Sample JM09/DC01 (NC 18959 46752) – TTG gneiss in the Laxfordian shear zone along strike from**
192 **the Scourie Dyke**

193 Sample JM09/DC01 is composed of c. 55% plagioclase, c. 25% quartz, c. 15% hornblende and c. 5%
194 biotite. Plagioclase crystals are subhedral, equant and 0.5-1 mm in diameter. They are thoroughly
195 sericitised and lamellar twinning and zoning are only rarely preserved. Quartz crystals are subhedral,
196 equant and 0.1-0.5 mm in diameter. They commonly aggregate to form a strong linear shape fabric
197 (Fig. 4f). Hornblende and biotite are also moderately aligned and parallel to this linear fabric.

198

199 **Sample JM08/29 (NC 18919 46758) – Deformed Scourie Dyke**

200 Sample JM08/29 is composed of c. 80% hornblende, c. 15% plagioclase and c. 5% clinopyroxene with
201 accessory opaques. Hornblende crystals range from subhedral elongate to anhedral rounded shapes,
202 0.2-1 mm in diameter, which aggregate together to define a strong linear fabric (Fig. 4g). The
203 pleochroic colour change happens at the same angle in most crystals indicating that they grew
204 during deformation. Plagioclase crystals are sub-millimetre in diameter and have an anhedral
205 rounded shape. The clinopyroxene occurs in elongate lenses aligned with the hornblende fabric. The
206 pyroxenes have a speckly altered appearance, occasionally pale-green in colour (Fig. 4h) with pink or

207 blue birefringence. They have a reaction rim of equant plagioclase crystals which generally have
208 well-defined concentric extinction (Fig. 4i). The clinopyroxenes are interpreted to be relict igneous
209 crystals which have been partially buffered from retrogression and deformation by their rims of
210 plagioclase.

211

212 **Sample JM08/30 (NC 18905 46760) – TTG gneiss from xenolith in Scourie Dyke**

213 Sample JM08/30 is composed of *c.* 40% plagioclase, *c.* 25% clinopyroxene, *c.* 20% quartz and *c.* 15%
214 hornblende. There is a compositional layering of mafic and felsic minerals at the thin section scale as
215 well as at the hand specimen scale but no linear fabrics. The plagioclase crystals are subhedral and
216 generally squarish, 0.5-2 mm in diameter; lamellar twinning and zoned extinction are commonly
217 preserved. Quartz crystals have anhedral irregular shapes and are 0.1-1 mm in size. Clinopyroxene
218 crystals are typically aggregated together in mafic bands and are pale green in colour with one
219 prominent cleavage (Fig. 4j). They are squarish and 1-2 mm in diameter with reaction rims of
220 aggregated equant sub-millimetre hornblende crystals. These rims are less than 1 mm wide and the
221 hornblende is locally associated with very small quartz blebs (Fig. 4k); some clinopyroxenes have
222 virtually no reaction rim and are in textural equilibrium with adjacent plagioclase (Fig. 4l). The
223 reaction rims record minor retrogression to amphibolite-facies. Retrogression in this sample has
224 been of a much lesser degree than in the four other samples.

225

226

227 **MINERAL CHEMISTRY**

228

229 In order to quantify the chemical changes that occurred with chemical reactions during the
230 different tectonothermal events indicated by petrographic observations, major element mineral
231 chemistry was conducted. Si, Ti, Fe, Al, Mn, Mg, Ca, Na, K and Ti oxides were measured using a
232 Cameca SX100 electron microprobe at the Natural History Museum, London. Operating conditions

233 were 15 kV accelerating voltage, a specimen current of 20 nA and a spot size of 1 micron. Silicate or
234 oxide standards were used, apart from for K for which a potassium bromide standard was used.
235 Detection limits were ~0.02-0.05 oxide weight percent. Full data are given in the Supplementary
236 Data; negligible core to rim zoning was observed and hence average values for each crystal are given
237 in Table 1.

238 Hornblende and plagioclase in the Scourie dyke samples JM08/28 and JM08/29 both
239 recrystallised during the Laxfordian tectonothermal event, although they are texturally different. The
240 abundance of Na₂O and CaO in plagioclase is almost identical in the two samples and major element
241 oxides in hornblende are also similar (Fig. 5, Table 1). Plagioclase in the TTG gneiss samples is much
242 more sodic and less calcic than in the Scourie Dyke samples, X_{An} of ~0.3 compared to 0.44.
243 Plagioclase in the xenolith (sample JM08/30) is slightly more calcic and less sodic than those in the
244 Inverian or Laxfordian assemblages X_{An} of 0.31-0.33 compared to 0.29 (Fig. 5, Table 1).
245 Clinopyroxenes in the xenolith have low K₂O (<0.1 wt.%) but the narrow hornblende trims around
246 them have higher K₂O (~1.3-1.5 wt.%) than the Laxfordian shear zone hornblendes and significantly
247 higher K₂O than Inverian shear zone hornblendes (~0.8 wt.%). TiO₂ shows a similar pattern between
248 samples than K₂O (Fig. 5, Table 1). Sieve-textured hornblende from the Inverian TTG gneiss is more
249 silicic (~43.5 wt.%) than narrow hornblende rims around clinopyroxene in the xenolith (~41-43 wt.%)
250 and hornblende laths recrystallized in the Laxfordian shear zone (42 wt.%).

251

252

253 **DISCUSSION**

254 The TTG gneiss xenolith contains a weak gneissic layering and equant clinopyroxenes with small
255 retrogression rims of hornblende. Whilst no orthopyroxene was found in thin section in this sample,
256 the presence of clinopyroxene clearly distinguishes it from the Inverian and Laxfordian metamorphic
257 assemblages observed in the surrounding TTG gneiss; the xenolith is therefore most likely a
258 relatively pristine Badcallian assemblage. The presence of narrow hornblende rims suggests that

259 very minor amphibolite-facies retrogression driven by fluid interaction has occurred within the
260 xenolith. Overall, the xenolith mineral assemblage contrasts with the TTG gneiss host rock adjacent
261 to the Scourie Dyke, which displays evidence of overprinting by tectonothermal events. This is
262 demonstrated by: (i) a planar fabric and the absence of pyroxene in the Inverian shear zone (sample
263 JM08/32), whereby original pyroxene has been completely retrogressed to sieve-textured
264 hornblende and quartz (e.g. Beach, 1974); (ii) the depletion of K and Ti in hornblende within sample
265 JM08/32, relative to the minor hornblende rims in the xenolith (Fig. 5c & f; and (iii) sericitised
266 feldspars and the development of planar and linear fabrics in sample JM09/DC01 consistent with its
267 position within the Laxfordian shear zone (e.g. Sheraton, *et al.*, 1973). The enrichment of Ti and K in
268 hornblende in the Laxfordian shear zone sample is attributed to an influx of K-rich fluids in the
269 Laxfordian, consistent with granite formation around the Laxford Shear Zone associated with partial
270 melting of local crust (Goodenough, *et al.*, 2010; Goodenough, *et al.*, 2013). It is important to note
271 that only the outer c. 1 m of the TTG xenolith displays a contact-parallel flaggy fabric.

272

273 **Xenolith source and transportation**

274 How did the Badcallian xenolith attain its current position in the Scourie Dyke in the Inverian- and
275 Laxfordian- age Laxford Shear Zone? One hypothesis is that it is in fact in-situ and is a low-strain
276 lacuna within the Inverian-age Laxford Shear Zone, which has been enveloped by the Scourie Dyke.
277 However, the proximity of its current location to Inverian deformation would suggest that even if the
278 xenolith had not been deformed during the Inverian, fluids circulating through the rocks would likely
279 have completely retrogressed its Badcallian assemblage. Badcallian gneisses that have been
280 statically retrogressed by Inverian fluids have very distinctive sieve-textured hornblende and quartz
281 pseudomorphs after pyroxene (e.g. MacDonald, *et al.*, 2015a), something not seen in the xenolith. As
282 a result, we favour the interpretation that the xenolith was entrained and transported by the NE-SW
283 oriented Scourie dyke from a position within the Badcallian TTG gneiss in the Assynt Terrane to the
284 southwest of its current location (Fig. 1b). We favour this source position because: (i) no TTG

285 gneisses with Badcallian granulite-facies assemblages are found to the northeast of the xenolith
286 locality (Fig. 1b) (e.g. Beach, 1974; Cohen, *et al.*, 1991; Whitehouse & Kemp, 2010); and (ii) the TTG
287 gneisses below the outcrop are still expected to lie within the steeply southwest-dipping Inverian-
288 age Laxford Shear Zone. This model therefore implies that dyke emplacement involved a significant
289 proportion of lateral, northwards-directed flow. Given that the xenolith is longer than the thickness
290 (~50 m) of the dyke, it is probable that: (i) they were transported with their long axes oriented NE-
291 SW, parallel to the dyke contact; and (ii) were subsequently rotated to a WNW-ESE orientation
292 during the development of the Laxfordian shear zone. The absence of stretching fabrics within the
293 xenolith implies that this potential reorientation occurred due to rotation rather than shearing.

294

295 **Post-emplacement dyke and xenolith evolution**

296 Our observations indicate that the Scourie Dyke and the TTG gneiss host rocks in and around the
297 Laxfordian shear zone were retrogressed to amphibolite-facies during the Laxfordian tectonothermal
298 event. This is supported by: (i) the hornblende aggregate lineation in the Scourie Dyke, which
299 unequivocally shows that it was deformed and retrogressed in the Laxfordian shear zone; (ii) static
300 retrogression of igneous pyroxene to hornblende and quartz, which demonstrates that the dyke was
301 also affected by the Laxfordian thermal regime and fluids beyond the shear zone; (iii) the complete
302 recrystallisation at amphibolite-facies of the TTG gneiss outside the dyke in the Inverian and
303 Laxfordian parts of the shear zone; and (iv) narrow hornblende rims around the xenolith
304 clinopyroxenes are closer in their chemistry, particularly Ti and K, to Laxfordian shear zone
305 hornblende than Inverian shear zone hornblende. The variation in plunge and plunge direction of the
306 lineation in the L-S tectonite fabric reflect the complication of having the xenolith in the Scourie
307 dyke. These chemical, mineralogical and textural modifications observed in both the Scourie dyke
308 and the TTG gneiss host rock indicate that H₂O-rich fluids circulated through these rocks during the
309 Laxfordian shear zone formation.

310 In contrast to those samples obtained from the Scourie dyke or the TTG gneiss host rock, our
311 results imply that the TTG gneiss xenolith was largely protected from retrogression and
312 recrystallization during the Laxfordian. This is supported by: (i) the preservation of a granulite-facies
313 assemblage in the TTG gneiss xenolith; (ii) the limited development of hornblende rims around
314 pyroxenes in the xenolith; and (iii) the restriction of deformation fabrics to the outer margin of the
315 xenolith. To explain this localized heterogeneity in the distribution of amphibolite-facies
316 retrogression during the Laxfordian, we invoke a model whereby preferential metamorphism,
317 reaction softening and strain localisation in the dyke restricted xenolith-fluid interactions.

318 We suggest that during the initial influx of fluid in the Laxfordian, likely coincident with the
319 formation of the Laxfordian shear zone (e.g. Beach, 1976), pyroxenes in both the Scourie Dyke and
320 the TTG gneiss xenolith started to undergo retrogression. This could explain the formation of small
321 hornblende rims on pyroxenes in the xenolith and the development of a contact-parallel fabric in the
322 outer margin of the xenolith generated by the onset of shear zone deformation. The fact that the
323 narrow hornblende rims around clinopyroxenes in the xenolith have similar concentrations of Ti and
324 K to the Laxfordian shear zone hornblende, and both are higher than the Inverian shear zone
325 hornblendes, supports this hypothesis. Because of the relatively large proportion of quartz, and
326 plagioclase to a lesser extent, in the TTG gneiss xenolith compared to the Scourie Dyke, we suggest
327 that the contemporaneous retrogression of both rock types progressed at a faster rate within the
328 dyke; i.e. there was a greater amount of pyroxene available that could retrogress to hornblende.
329 Importantly, these mineralogical and chemical changes from pyroxene to hornblende could change
330 the physical properties of the rock. In particular, this transformation can be considered a form of
331 reaction softening (e.g. White & Knipe, 1978; Wibberley, 1999; Stünitz & Tullis, 2001; Holyoke &
332 Tullis, 2006a; Holyoke & Tullis, 2006b). Similarly, the formation of hornblende aggregates in sample
333 JM09/DC01 (the Laxfordian shear zone) can instigate a mineral preferred orientation and thereby
334 'weaken' the rock. Plagioclase alteration to sericite (e.g., sample JM09/DC01), a much weaker
335 phyllosilicate, also induces reaction softening. Additionally, many studies have documented that the

336 occurrence of reaction softening processes in metamorphic rocks can focus strain, promoting the
337 formation of shear zones (e.g. Keller, *et al.*, 2004; Whitmeyer & Wintsch, 2005; Oliot, *et al.*, 2010).
338 We suggest that the greater propensity for reaction softening retrogression of pyroxene to
339 amphibole in the Scourie Dyke, compared to the more felsic TTG gneiss xenolith, would have
340 resulted in strain localisation in the dyke. In conjunction with field and microstructural work
341 demonstrating that the Scourie dykes deform preferentially to the TTG gneisses (Pearce, *et al.*,
342 2011), this strain localisation may explain why strong planar and linear fabrics are developed in the
343 dyke but only at the outer margin of the TTG gneiss xenolith.

344 The increase in shear fabric intensity at the dyke margins suggests strain may also have
345 preferentially accrued along the dyke margins. This supports the observations of Wheeler *et al.*,
346 (1987) who showed that Laxfordian deformation was concentrated along dyke margins at Diabaig in
347 the southern part of the mainland Lewisian Gneiss Complex outcrop. Park *et al.*, (1987) suggested
348 that as deformation progressed, strain initially localised at the dyke margins would start to affect the
349 whole of the dyke. Strain localisation can control fluid flow and is here interpreted to have been an
350 important process in directing fluids around, but not through, the xenolith. This is consistent with
351 previous studies, which have shown that the Laxfordian shear zones throughout the Lewisian Gneiss
352 Complex acted as preferential fluid flow pathways during the Laxfordian tectonothermal event
353 (Beach, 1973; Beach, 1976). Strain localisation leading to directed fluid flow is a common
354 phenomenon and many examples are discussed in the literature (e.g. Goldblum & Hill, 1992; Ring,
355 1999; Babiker & Gudmundsson, 2004; Clark, *et al.*, 2005; Blenkinsop & Kadzviti, 2006; Tartese, *et al.*,
356 2012). Whilst we acknowledge that these are a near-surface analogue for our mid-crustal study in
357 the Lewisian Gneiss Complex, the general principal of dyke-fluid interaction geometry is the same.
358 Several studies have similarly demonstrated that crystallised igneous intrusions may deflect
359 migrating fluids along their margins (Rateau, *et al.*, 2013; Grove, 2014; Jacquemyn, *et al.*, 2014). The
360 proposed model (Fig. 6) implies that the interplay between the processes of reaction softening,
361 strain localisation (e.g., shear zone development) and directed fluid flow resulted in the xenolith

362 escaping amphibolite-facies retrogression. This combination of factors clearly has the potential to
363 allow preservation of early metamorphic assemblages and fabrics in polymetamorphic terranes,
364 specifically in dyke-hosted country rock xenoliths.

365

366

367 **CONCLUSIONS**

368 This study illustrates an example of a mafic dyke acting as a barrier to metamorphic overprinting of
369 entrained country rock xenoliths from the Archaean-Palaeoproterozoic Lewisian Gneiss Complex of
370 Northwest Scotland. Field mapping and petrographic analysis show that a tonalite-trondhjemite-
371 granodiorite (TTG) gneiss xenolith entrained in a member of the Scourie Dyke Swarm retains a
372 Badcallian granulite-facies pyroxene-bearing mineral assemblage and coarse gneissic layering with
373 no lineation, whereas the dyke and surrounding country rock display evidence of Inverian and
374 Laxfordian amphibolite-facies overprinting. We suggest that the xenolith was entrained by the dyke
375 from an area, likely to the SW of the current exposure from an area unaffected by the Inverian
376 tectonothermal event. Mineral chemistry highlights some of the chemical changes that have
377 occurred within the major minerals due to the influx of fluid that resulted in retrogressive
378 metamorphic reactions. We interpret that the xenolith escaped Laxfordian retrogression through an
379 interplay of factors: reaction softening, strain localisation and directed fluid flow. Retrogressive
380 reaction softening, along with planes of weakness such as the pre-existing Inverian fabric and gneiss-
381 dyke contacts, localised strain around but not within the xenolith. Strain localisation generated
382 preferential flow pathways for fluids, principally along the shear zone. In the Lewisian Gneiss
383 Complex, areas with early metamorphic assemblages and fabrics survive but in many
384 polymetamorphic terranes this is not the case. This study shows that gneissic country rock xenoliths
385 in mafic dykes could help to unravel polymetamorphic histories of basement gneiss complexes
386 where the majority of the country rock has been overprinted, obscuring early tectonothermal
387 events.

388

389

390 **ACKNOWLEDGEMENTS**

391

392 The fieldwork was carried out under UK Natural Environment Research Council DTG NE/G523855/1
393 and British Geological Survey CASE Studentship 2K08E010 to JMM. John Wheeler and Quentin
394 Crowley assisted with fieldwork. Alan Boyle is thanked for taking the photomicrographs. John Spratt
395 assisted with mineral chemistry analyses at the Natural History Museum. Comments from Maarten
396 Krabbendam on an early draft considerably improved this manuscript. KG publishes with the
397 permission of the Executive Director of the British Geological Survey.

398

399 **Figure Captions**

400 **Fig. 1.** Location maps. (a) Outcrop of the Lewisian Gneiss Complex in Northwest Scotland, inset map
401 shows location in the wider British & Irish Isles. (b) Location of the locality investigated in this study
402 relative to the major geological structure in the area, the Laxford Shear Zone.

403 **Fig. 2.** Detailed field map of lithology and structure at the locality with sample locations marked.

404 **Fig. 3.** (a) Photograph of deformed Scourie dyke with inset sketch showing L-S tectonite nature of
405 fabric. (b) Field sketch showing onset of deformation in the Scourie dyke at the margin of the
406 Laxfordian shear zone with photographs of fabric styles. (c) Detail map of TTG gneiss xenolith within
407 the dyke, sample location marked.

408 **Fig. 4.** Photomicrographs of the samples analysed petrographically. (a) Quartz mineral aggregate
409 lineation in sample JM08/32, TTG gneiss with Inverian fabric. (b) Elongate sieve-textured hornblende
410 and quartz pseudomorphs after pyroxene in sample JM08/32. (c) Clumps of weakly aligned biotite
411 laths, roughly aligned with the quartz aggregate lineation. (d) Pseudomorphs after pyroxene of
412 sieve-textured hornblende and quartz in sample JM08/28, undeformed Scourie dyke; the edges of
413 the pseudomorphs are dominated by hornblende with more quartz in the cores. (e) Plagioclase

414 showing well-preserved lamellar twinning and zoned extinction in sample JM08/28. (f) Quartz
415 mineral aggregate lineation in sample JM09/DC01, TTG gneiss in the Laxfordian shear zone along
416 strike from the Scourie dyke. (g) Hornblende crystals aggregated to form a strong lineation in sample
417 JM08/29, the deformed Scourie dyke. (h) Elongate lenses of relict clinopyroxene in sample JM08/29.
418 (i) A reaction rim of equant plagioclase crystals around the clinopyroxene in (h). (j) Clinopyroxene
419 crystals aggregated together in sample JM08/30, TTG gneiss from xenolith in Scourie dyke. (k)
420 Clinopyroxene with rim of aggregated hornblende crystals in sample JM08/30. (l) Clinopyroxene with
421 no hornblende rim in textural equilibrium with plagioclase in sample JM08/30.

422 **Fig. 5.** Plots of mineral chemistry data (in weight percentage cation oxide) from the samples
423 analysed in this study. (a) Na vs CaO in plagioclase. (b) Mg vs Si in hornblende. (c) Ti vs Si in
424 hornblende. (d) Na vs Si in hornblende. (e) Mn vs Si in hornblende. (f) K vs Si in hornblende.

425 **Fig. 6.** Schematic maps illustrating the tectonothermal evolution of the xenolith and surrounding
426 rocks.

427

428

429 Table Captions

430

431 **Table 1.** Mineral chemistry data. Cation oxide values in weight percent. Cation values in number of
432 ions per formula unit; number of oxygens used in this calculation: hornblende = 23, clinopyroxene = 6,
433 plagioclase = 8, biotite = 11. “plag” denotes plagioclase, “cpx” clinopyroxene, “bt” biotite and “hbl”
434 hornblende.

435

436 REFERENCES

437 Babiker, M. & Gudmundsson, A., 2004. The effects of dykes and faults on groundwater flow in an
438 arid land: the Red Sea Hills, Sudan. *Journal of Hydrology*, **297**(1-4), 256-273.
439 Beach, A., 1973. Mineralogy of High-Temperature Shear Zones at Scourie, NW Scotland. *Journal of*
440 *Petrology*, **14**(2), 231-248.
441 Beach, A., 1974. Amphibolitization of Scourian granulites. *Scottish Journal of Geology*, **10**(1), 35-43.

442 Beach, A., 1976. Interrelations of Fluid Transport, Deformation, Geochemistry and Heat-Flow in Early
443 Proterozoic Shear Zones in Lewisian Complex. *Philosophical Transactions of the Royal Society*
444 *of London Series a-Mathematical Physical and Engineering Sciences*, **280**(1298), 569-604.

445 Blenkinsop, T. G. & Kadzviti, S., 2006. Fluid flow in shear zones: insights from the geometry and
446 evolution of ore bodies at Renco gold mine, Zimbabwe. *Geofluids*, **6**(4), 334-345.

447 British Geological Survey, 2007. Assynt. Scotland Special Sheet. Bedrock. 1:50000 Geological Series
448 (ed Survey, B. G.), Keyworth, Nottingham.

449 Clark, C., Mumm, A. S. & Faure, K., 2005. Timing and nature of fluid flow and alteration during
450 Mesoproterozoic shear zone formation, Olary Domain, South Australia. *Journal of*
451 *Metamorphic Geology*, **23**(3), 147-164.

452 Cohen, A. S., Onions, R. K. & O' Hara, M. J., 1991. Chronology and Mechanism of Depletion in
453 Lewisian Granulites. *Contributions to Mineralogy and Petrology*, **106**(2), 142-153.

454 Coward, M. & Park, R. G., 1987. The role of mid-crustal shear zones in the Early Proterozoic evolution
455 of the Lewisian. In: *Evolution of the Lewisian and Comparable Precambrian High-Grade*
456 *Terrains* (eds Park, R. G. & Tarney, J.), Blackwells.

457 Crowley, Q. G., Key, R. & Noble, S. R., 2014. High-precision U–Pb dating of complex zircon from the
458 Lewisian Gneiss Complex of Scotland using an incremental CA-ID-TIMS approach. *Gondwana*
459 *Research*, **In Press**.

460 Davies, J. H. F. L. & Heaman, L., 2014. New U-Pb baddeleyite and zircon ages for the Scourie dyke
461 swarm: A long-lived large igneous province with implications for the Paleoproterozoic
462 evolution of NW Scotland. *Precambrian Research*, **249**, 180-198.

463 Evans, C. R., 1965. Geochronology of the Lewisian Basement near Lochinver, Sutherland. *Nature*,
464 **204**, 638-641.

465 Friend, C. R. L. & Kinny, P. D., 1995. New Evidence for Protolith Ages of Lewisian Granulites,
466 Northwest Scotland. *Geology*, **23**(11), 1027-1030.

467 Goldblum, D. R. & Hill, M. L., 1992. Enhanced Fluid-Flow Resulting from Competence Contrast within
468 a Shear Zone - the Garnet Ore Zone at Gore Mountain, Ny. *Journal of Geology*, **100**(6), 776-
469 782.

470 Goodenough, K. M., Crowley, Q., Krabbendam, M. & Parry, S. F., 2013. New U-Pb age constraints for
471 the Laxford Shear Zone, NW Scotland: evidence for tectono-magmatic processes associated
472 with the formation of a Palaeoproterozoic supercontinent. *Precambrian Research*, **223**, 1-19.

473 Goodenough, K. M., Park, R. G., Krabbendam, M., Myers, J. S., Wheeler, J., Loughlin, S. C., Crowley,
474 Q. G., Friend, C. R. L., Beach, A., Kinny, P. D. & Graham, R. H., 2010. The Laxford Shear Zone:
475 an end-Archaean terrane boundary? In: *Continental Tectonics and Mountain Building* (eds
476 Law, R. D., Butler, R. W. H., Holdsworth, R. E., Krabbendam, M. & Strachan, R. A.) *Special*
477 *Publications*, Geological Society, London.

478 Grove, C., 2014. *Direct and Indirect Effects of Flood Basal Volcanism on Reservoir Quality Sandstone*.
479 Unpub. Ph.D. Thesis, Durham University.

480 Holyoke, C. W. & Tullis, J., 2006a. Formation and maintenance of shear zones. *Geology*, **34**(2), 105-
481 108.

482 Holyoke, C. W. & Tullis, J., 2006b. Mechanisms of weak phase interconnection and the effects of
483 phase strength contrast on fabric development. *Journal of Structural Geology*, **28**(4), 621-
484 640.

485 Hoskin, P. W. O. & Schaltegger, U., 2003. The composition of zircon and igneous and metamorphic
486 petrogenesis. In: *Zircon* (eds Hanchar, J. & Hoskin, P. W. O.), pp. 27-62, Mineralogical Society
487 of America and The Geochemical Society.

488 Jacquemyn, C., El Desouky, H., Hunt, D., Casini, G. & Swennen, R., 2014. Dolomitization of the
489 Latemar platform: Fluid flow and dolomite evolution. *Marine and Petroleum Geology*, **55**(0),
490 43-67.

491 Johnson, T. E. & White, R. W., 2011. Phase equilibrium constraints on conditions of granulite-facies
492 metamorphism at Scourie, NW Scotland. *Journal of the Geological Society*, **168**(1), 147-158.

493 Keller, L. M., Abart, R., Stünitz, H. & De Capitani, C., 2004. Deformation, mass transfer and mineral
494 reactions in an eclogite facies shear zone in a polymetamorphic metapelite (Monte Rosa
495 nappe, western Alps). *Journal of Metamorphic Geology*, **22**(2), 97-118.

496 Kinny, P. D., Friend, C. R. L. & Love, G. J., 2005. Proposal for a terrane-based nomenclature for the
497 Lewisian Gneiss Complex of NW Scotland. *Journal of the Geological Society*, **162**, 175-186.

498 MacDonald, J. M., Goodenough, K. M., Wheeler, J., Crowley, Q., Harley, S. L., Mariani, E. & Tatham,
499 D., 2015a. Temperature–time evolution of the Assynt Terrane of the Lewisian Gneiss
500 Complex of Northwest Scotland from zircon U-Pb dating and Ti thermometry. *Precambrian
501 Research*, **260**(0), 55-75.

502 MacDonald, J. M., Goodenough, K. M., Wheeler, J., Crowley, Q., Harley, S. L., Mariani, E. & Tatham,
503 D., 2015b. Temperature–time evolution of the Assynt Terrane of the Lewisian Gneiss
504 Complex of Northwest Scotland from zircon U-Pb dating and Tithermometry. *Precambrian
505 Research*, **260**, 55-75.

506 MacDonald, J. M., Wheeler, J., Harley, S. L., Mariani, E., Goodenough, K. M., Crowley, Q. & Tatham,
507 D., 2013. Lattice distortion in a zircon population and its effects on trace element mobility
508 and U–Th–Pb isotope systematics: examples from the Lewisian Gneiss Complex, northwest
509 Scotland. *Contributions to Mineralogy and Petrology*, **166**(1), 21-41.

510 Olliot, E., Goncalves, P. & Marquer, D., 2010. Role of plagioclase and reaction softening in a
511 metagranite shear zone at mid-crustal conditions (Gotthard Massif, Swiss Central Alps).
512 *Journal of Metamorphic Geology*, **28**(8), 849-871.

513 Park, R. G., 1970. Observations on Lewisian Chronology. *Scottish Journal of Geology*, **6**(4), 379-399.

514 Park, R. G., 2005. The Lewisian terrane model: a review. *Scottish Journal of Geology*, **41**, 105-118.

515 Park, R. G., Crane, A. & Niamatullah, M., 1987. Early Proterozoic structure and kinematic evolution of
516 the southern mainland Lewisian. In: *Evolution of the Lewisian and Comparable Precambrian
517 High-Grade Terrains* (eds Park, R. G. & Tarney, J.).

518 Peach, B. N., Horne, J., Gunn, W., Clough, C. T. & Hinxman, L. W., 1907. *The Geological Structure of
519 the Northwest Highlands of Scotland*. H.M.S.O., London.

520 Pearce, M. A., Wheeler, J. & Prior, D. J., 2011. Relative strength of mafic and felsic rocks during
521 amphibolite facies metamorphism and deformation. *Journal of Structural Geology*, **33**(4),
522 662-675.

523 Rateau, R., Schofield, N. & Smith, M., 2013. The potential role of igneous intrusions on hydrocarbon
524 migration, West of Shetland. *Petroleum Geoscience*, **19**(3), 259-272.

525 Ring, U., 1999. Volume loss, fluid flow, and coaxial versus noncoaxial deformation in retrograde,
526 amphibolite facies shear zones, northern Malawi, east-central Africa. *Geological Society of
527 America Bulletin*, **111**(1), 123-142.

528 Sheraton, J. W., Tarney, J., Wheatley, T. J. & Wright, A. E., 1973. The structural history of the Assynt
529 district. In: *The Early Precambrian of Scotland and Related Rocks of Greenland* (eds Park, R.
530 G. & Tarney, J.), University of Keele.

531 Stünitz, H. & Tullis, J., 2001. Weakening and strain localization produced by syn-deformational
532 reaction of plagioclase. *International Journal of Earth Sciences*, **90**(1), 136-148.

533 Sutton, J. & Watson, J., 1951. The pre-Torridonian metamorphic history of the Loch Torridon and
534 Scourie areas in the North-West Highlands, and its bearing on the chronological classification
535 of the Lewisian. *Quarterly Journal of the Geological Society*, **106**, 241-296.

536 Tarney, J. & Weaver, B. L., 1987. Geochemistry of the Scourian Complex: petrogenesis and tectonic
537 models. In: *Evolution of the Lewisian and Comparable Precambrian High-Grade Terrains* (eds
538 Park, R. G. & Tarney, J.), Blackwells.

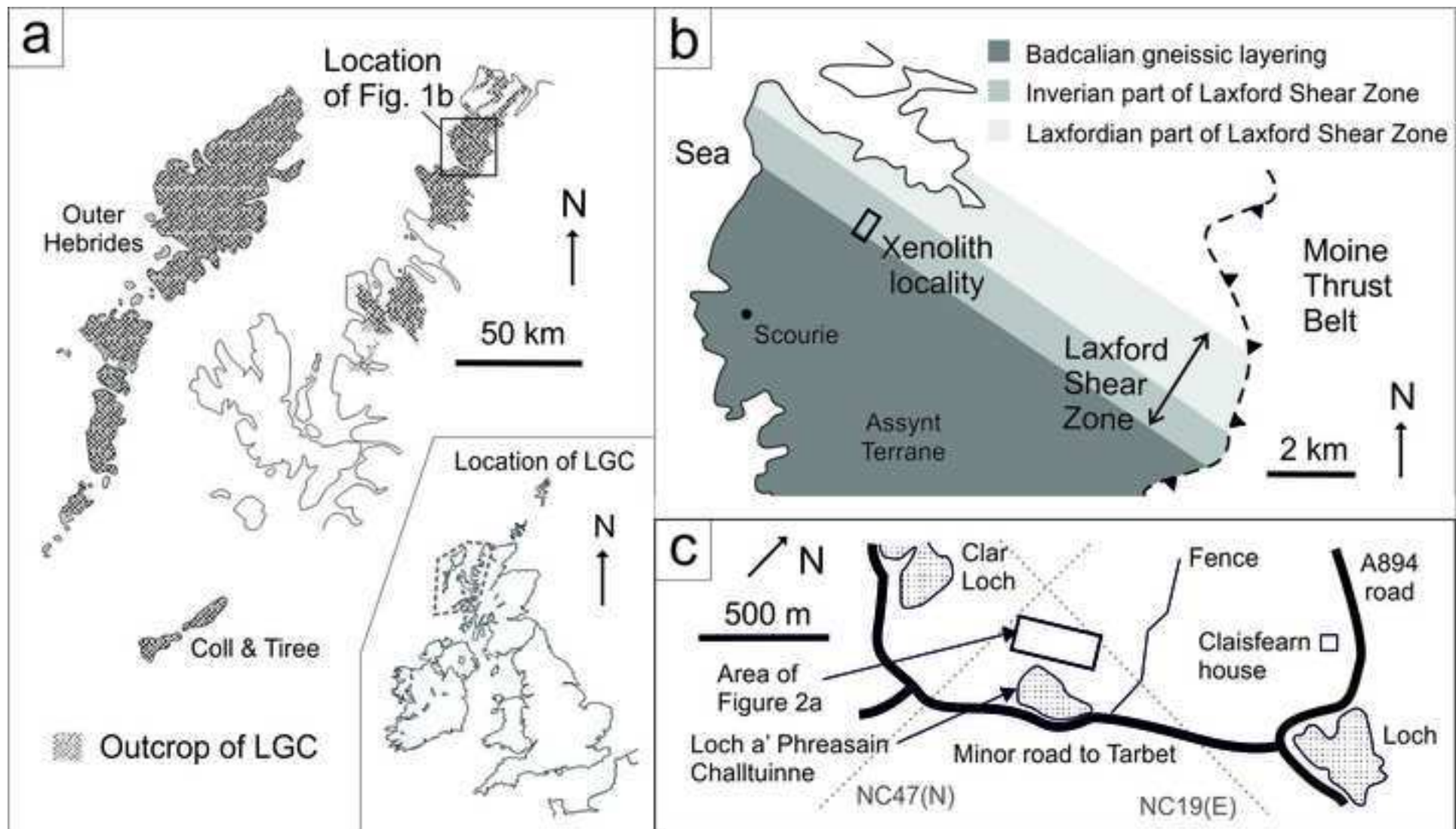
539 Tartese, R., Boulvais, P., Pujol, M., Chevalier, T., Paquette, J. L., Ireland, T. R. & Deloule, E., 2012.
540 Mylonites of the South Armorican Shear Zone: Insights for crustal-scale fluid flow and water-
541 rock interaction processes. *Journal of Geodynamics*, **56-57**, 86-107.

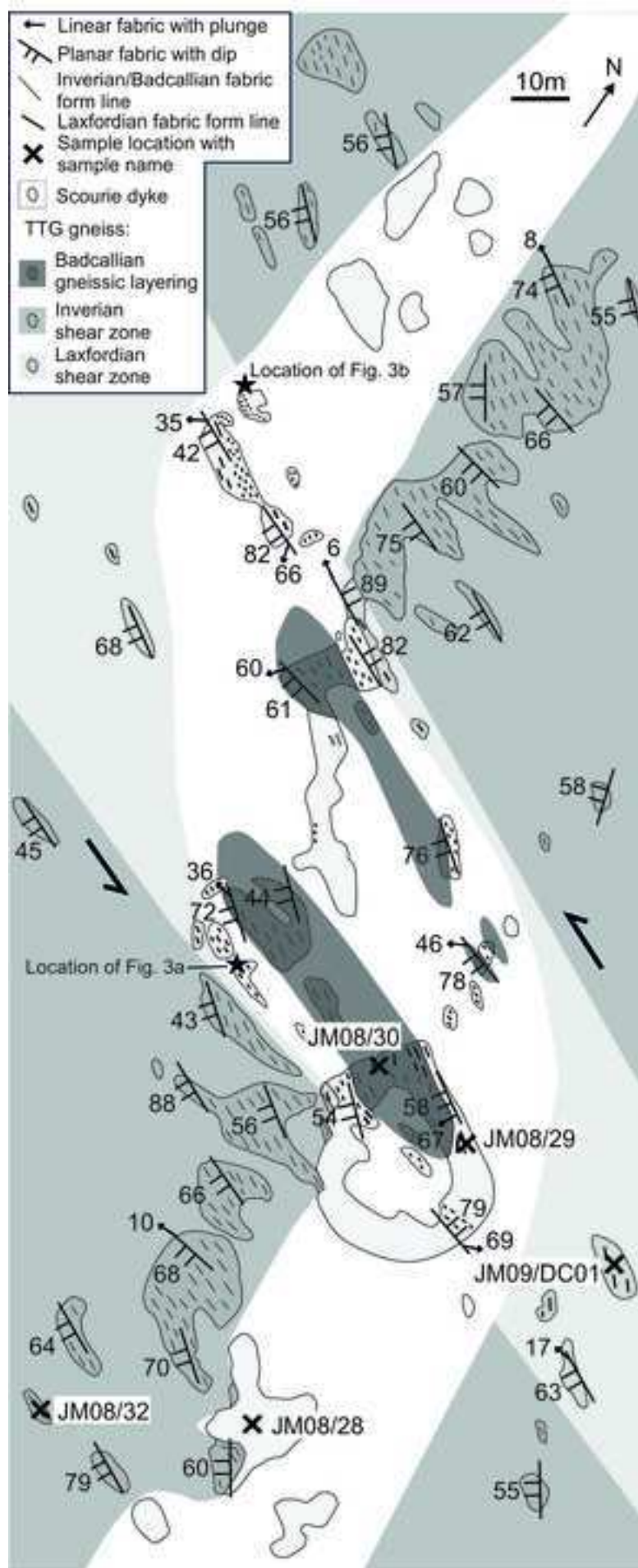
- 542 Wheeler, J., Windley, B. F. & Davies, F. B., 1987. Internal evolution of the major Precambrian shear
543 belt at Torridon, NW Scotland. In: *Evolution of the Lewisian and Comparable Precambrian*
544 *High-Grade Terrains* (eds Park, R. G. & Tarney, J.), Blackwells.
- 545 White, J. C., 2004. Instability and localization of deformation in lower crust granulites, Minas fault
546 zone, Nova Scotia, Canada. *Flow Processes in Faults and Shear Zones*, **224**, 25-37.
- 547 White, S. H. & Knipe, R. J., 1978. Transformation- and reaction-enhanced ductility in rocks. *Journal of*
548 *the Geological Society*, **135**(5), 513-516.
- 549 Whitehouse, M. & Kemp, A. I. S., 2010. On the difficulty of assigning crustal residence, magmatic
550 protolith and metamorphic ages to Lewisian granulites: constraints from combined in-situ U-
551 Pb and Lu-Hf isotopes. In: *Continental Tectonics and Mountain Building: The Legacy of Peach*
552 *and Horne* (eds Law, R. D., Butler, R. W. H., Holdsworth, R. E., Krabbendam, M. & Strachan,
553 R. A.) *Special Publications*, The Geological Society Publishing House.
- 554 Whitmeyer, S. J. & Wintsch, R. P., 2005. Reaction localization and softening of texturally hardened
555 mylonites in a reactivated fault zone, central Argentina. *Journal of Metamorphic Geology*,
556 **23**(6), 411-424.
- 557 Wibberley, C., 1999. Are feldspar-to-mica reactions necessarily reaction-softening processes in fault
558 zones? *Journal of Structural Geology*, **21**(8-9), 1219-1227.
- 559 Wynn, T. J., 1995. Deformation in the mid to lower continental crust: analogues from Proterozoi
560 shear zones in NW Scotland. In: *Early Precambrian Processes* (eds Coward, M. P. & Ries, A.
561 C.), The Geological Society Publishing House.

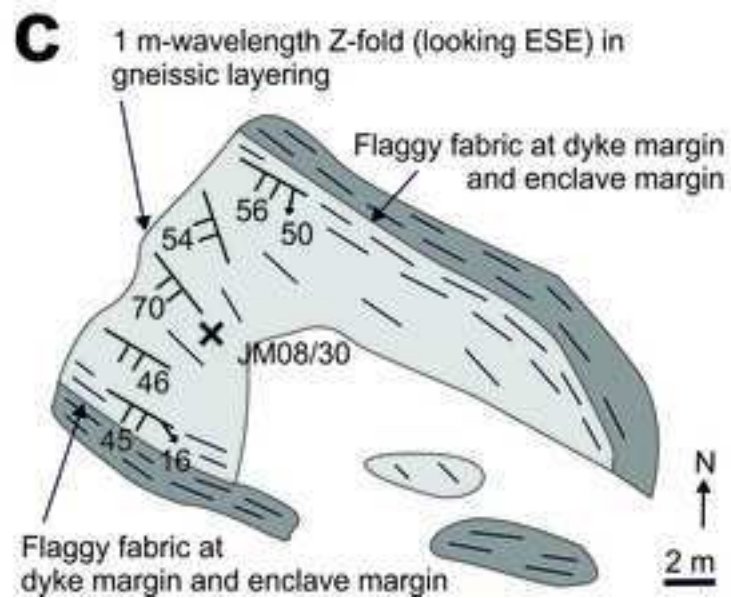
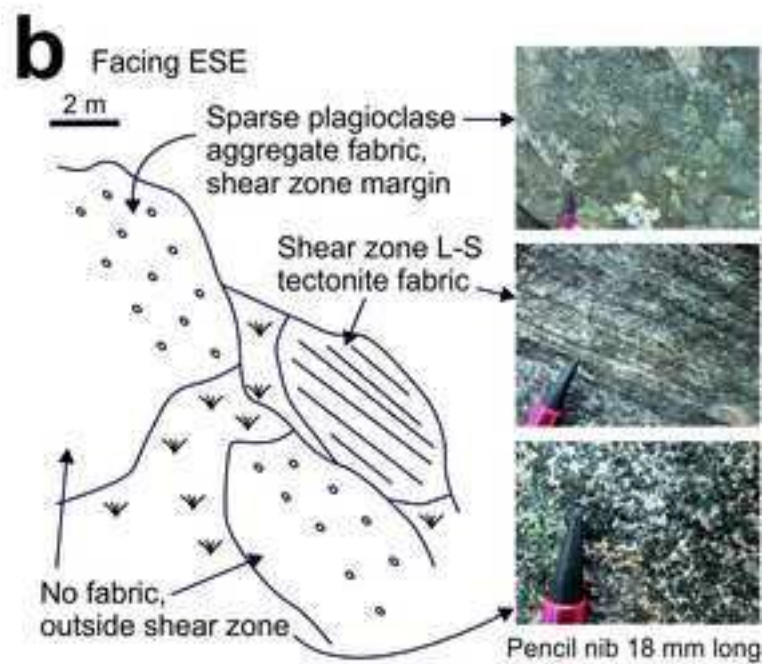
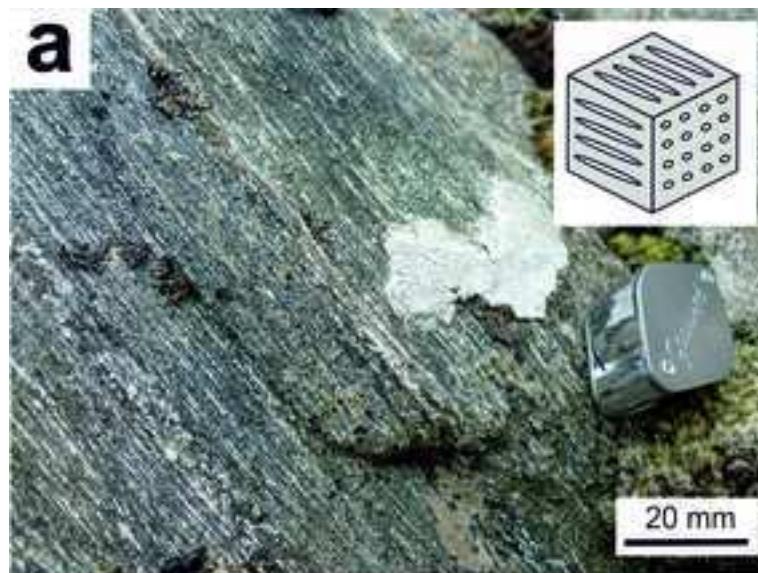
562

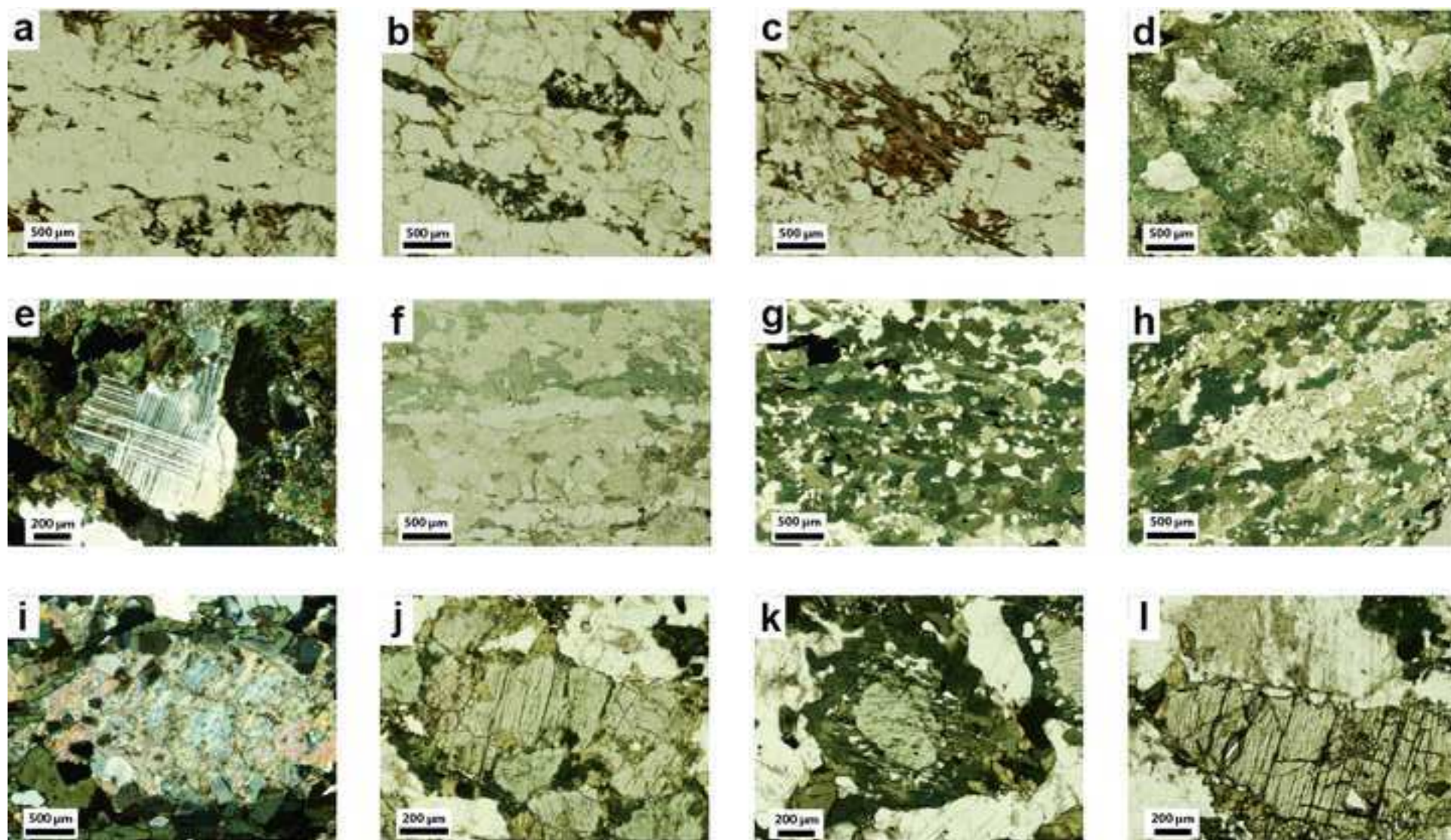
Sample	JM08/28			JM08/29	JM08/30		JM08/32	JM09/DC01	JM08/30			JM08/32	
Mineral	plag	plag	plag	plag	plag	plag	plag	plag	cpx	cpx	cpx	cpx	bt
SiO ₂	57.14	57.41	58.22	57.17	59.26	61.50	61.72	62.63	50.31	51.39	51.77	50.48	34.98
TiO ₂	0.00	0.02	0.02	0.01	0.03	0.00	0.00	0.00	0.14	0.07	0.10	0.11	2.46
Al ₂ O ₃	27.62	27.51	27.68	26.65	25.14	25.08	25.02	24.62	2.02	1.27	1.46	1.59	16.85
FeO	0.24	0.09	0.08	0.18	0.09	0.04	0.02	0.05	11.10	9.87	10.52	10.59	20.78
MnO	0.00	0.01	0.00	0.00	0.00	0.00	0.00	0.00	0.56	0.57	0.59	0.58	0.13
MgO	0.07	0.00	0.00	0.00	0.00	0.00	0.00	0.00	11.36	12.09	11.63	11.64	11.63
CaO	9.31	9.33	9.43	9.12	7.10	6.62	6.36	6.10	23.17	24.17	24.02	23.88	0.11
Na ₂ O	6.45	6.61	6.57	6.57	7.92	8.13	8.43	8.33	0.71	0.62	0.67	0.68	0.16
K ₂ O	0.24	0.07	0.07	0.07	0.23	0.24	0.06	0.10	0.10	0.00	0.01	0.02	6.93
Cr ₂ O ₃	0.01	0.00	0.00	0.00	0.00	0.00	0.01	0.00	0.05	0.04	0.04	0.06	0.05
Total	101.09	101.08	102.07	99.77	99.77	101.62	101.64	101.85	99.56	100.14	100.87	99.68	94.32
Si	2.54	2.55	2.56	2.57	2.66	2.70	2.70	2.73	1.93	1.95	1.95	1.93	2.68
Ti	0.00	0.00	0.00	0.00	0.00	0.00	0.00	0.00	0.00	0.00	0.00	0.00	0.14
Al	1.45	1.44	1.43	1.41	1.33	1.30	1.29	1.26	0.09	0.06	0.06	0.07	1.52
Fe	0.01	0.00	0.00	0.01	0.00	0.00	0.00	0.00	0.36	0.31	0.33	0.34	1.33
Mn	0.00	0.00	0.00	0.00	0.00	0.00	0.00	0.00	0.02	0.02	0.02	0.02	0.01
Mg	0.00	0.00	0.00	0.00	0.00	0.00	0.00	0.00	0.65	0.68	0.65	0.66	1.33
Ca	0.44	0.44	0.44	0.44	0.34	0.31	0.30	0.28	0.95	0.98	0.97	0.98	0.01
Na	0.56	0.57	0.56	0.57	0.69	0.69	0.72	0.70	0.05	0.05	0.05	0.05	0.02
K	0.01	0.00	0.00	0.00	0.01	0.01	0.00	0.00	0.00	0.00	0.00	0.00	0.68
Cr	0.00	0.00	0.00	0.00	0.00	0.00	0.00	0.00	0.00	0.00	0.00	0.00	0.00
X _{Mg}									0.65	0.69	0.66	0.66	0.50
X _{An}	0.44	0.44	0.44	0.43	0.33	0.31	0.29	0.29					
Total Cations	5.01	5.01	5.00	5.00	5.03	5.01	5.01	4.99	4.05	4.04	4.03	4.05	7.73

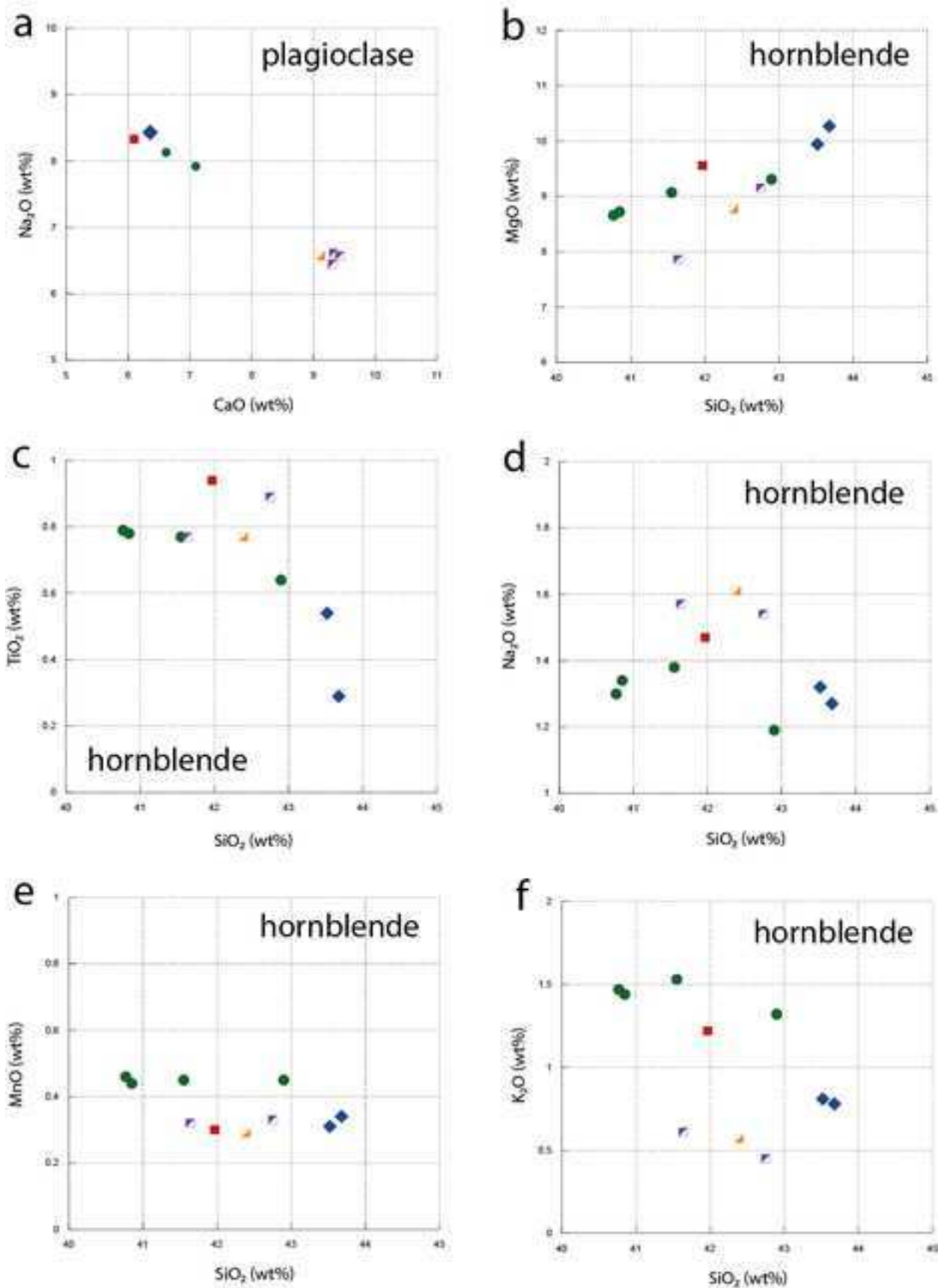
Sample	JM08/28			JM08/29		JM08/30			JM08/32		JM09/DC01
Mineral	hbl	hbl	hbl	hbl	hbl	hbl	hbl	hbl	hbl	hbl	hbl
Texture	sieve- texture	sieve- texture	sieve- texture	rim around remnant cpx?	rim round cpx	rim round cpx	rim round cpx	rim round cpx	sieve- texture	sieve- texture	lath
SiO ₂	42.75	41.64	45.31	42.39	40.85	42.90	41.55	40.77	43.68	43.52	41.97
TiO ₂	0.89	0.77	0.48	0.77	0.78	0.64	0.77	0.79	0.29	0.54	0.94
Al ₂ O ₃	11.05	12.42	9.46	12.63	11.49	9.84	12.11	11.38	11.23	11.12	11.63
FeO	18.85	20.44	18.30	18.53	19.73	18.30	18.29	19.82	17.51	17.70	18.33
MnO	0.33	0.32	0.31	0.29	0.44	0.45	0.45	0.46	0.34	0.31	0.30
MgO	9.15	7.86	10.19	8.77	8.72	9.31	9.07	8.66	10.27	9.94	9.56
CaO	11.94	11.74	12.18	11.33	12.10	13.02	12.16	12.14	11.91	11.89	11.94
Na ₂ O	1.54	1.57	1.19	1.61	1.34	1.19	1.38	1.30	1.27	1.32	1.47
K ₂ O	0.45	0.61	0.37	0.57	1.44	1.32	1.53	1.47	0.78	0.81	1.22
Cr ₂ O ₃	0.04	0.04	0.13	0.03	0.07	0.05	0.11	0.06	0.03	0.04	0.05
Total	97.22	97.64	98.12	97.23	97.07	97.10	97.51	96.96	97.45	97.33	97.69
Si	6.52	6.37	6.78	6.43	6.33	6.58	6.35	6.33	6.58	6.58	6.39
Ti	0.10	0.09	0.05	0.09	0.09	0.07	0.09	0.09	0.03	0.06	0.11
Al	1.98	2.24	1.67	2.26	2.10	1.78	2.18	2.08	2.00	1.98	2.09
Fe	2.40	2.62	2.29	2.35	2.56	2.35	2.34	2.57	2.21	2.24	2.33
Mn	0.04	0.04	0.04	0.04	0.06	0.06	0.06	0.06	0.04	0.04	0.04
Mg	2.08	1.79	2.28	1.98	2.01	2.13	2.07	2.00	2.31	2.24	2.17
Ca	1.95	1.92	1.95	1.84	2.01	2.14	1.99	2.02	1.92	1.93	1.95
Na	0.46	0.47	0.35	0.47	0.40	0.35	0.41	0.39	0.37	0.39	0.43
K	0.09	0.12	0.07	0.11	0.29	0.26	0.30	0.29	0.15	0.16	0.24
Cr	0.00	0.00	0.02	0.00	0.01	0.01	0.01	0.01	0.00	0.00	0.01
X _{Mg}	0.46	0.41	0.50	0.46	0.44	0.48	0.47	0.44	0.51	0.50	0.48
Total Cations	15.62	15.67	15.50	15.59	15.85	15.73	15.79	15.85	15.62	15.61	15.74



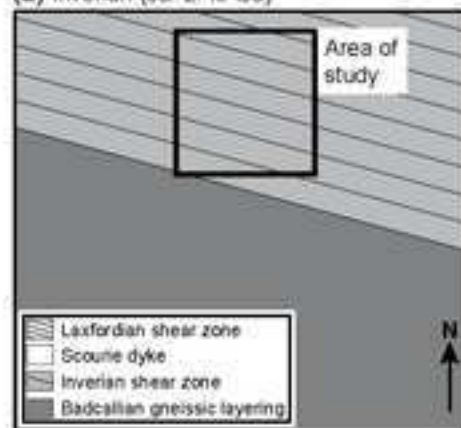
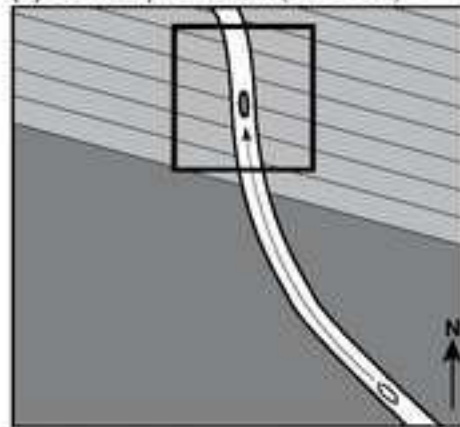
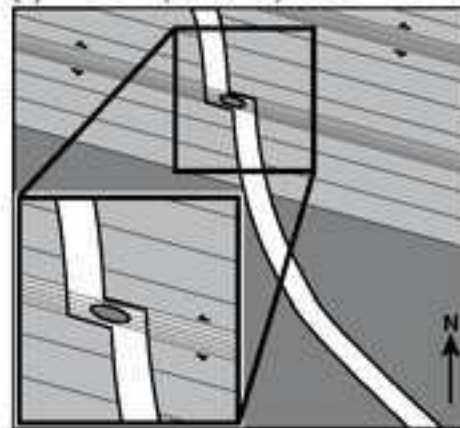








- ◆ JM08/28 - undefomed Scourie Dyke
 - ◆ JM08/29 - defomed Scourie Dyke
 - JM08/30 - TTG gneiss from xenolith in Scourie Dyke (hornblendes are narrow rims around clinopyroxenes)
- JM09/DC01 - TTG gneiss with Laxfordian fabric (hornblende is fabric-forming lath)
 - ◆ JM08/32 - TTG gneiss with Inverian fabric (hornblendes are sieve-textured)

(a) Inverian (ca. 2.48 Ga)**(b) Scourie dyke intrusion (ca. 2.4 Ga)****(c) Laxfordian (ca. 1.7 Ga)**



[Click here to access/download](#)

Dataset

Supplementary Data Tables.pdf

